

Two-Stream Instability in a Paraxial Quantum Fluid of Light

João D. Rodrigues^{1,*} and José T. Mendonça¹

¹*Instituto de Plasmas e Fusão Nuclear, Instituto Superior Técnico,
Universidade de Lisboa, 1049-001 Lisbon, Portugal*

Under paraxial propagation, light in bulk nonlinear media is known to behave as a quantum fluid, described by a nonlinear Schrödinger equation formally equivalent to the Gross-Pitaevskii model of a weakly interacting Bose gas. Photon-photon interactions, mediated by third order optical nonlinearities, are at the origin of superfluidity and other quantum-like phenomena. Here, we develop an optical hydrodynamic theory to describe the onset of a kinetic instability when two fluids of light with different flow speeds interact via the optical nonlinearity. The experimental observation of such effects is also discussed in detail. The class of instabilities described here may provide a route towards the investigation of quantum turbulence, structure formation and general many-body and out-of-equilibrium dynamics in the quantum superfluid regime.

Introduction - Quantum gases owe most of their peculiar nature to the wave-like character of matter emerging at low temperatures, when the de Broglie wavelength is larger than the inter-particle distance. Here, an emergent macroscopic wavefunction describes the entire collection of particles, such as in the case of atomic Bose-Einstein condensates [1–3], where superfluidity [4–7] and quantum turbulence [8–12] witness the exotic nature of these systems. Interestingly, quantum behavior is also expected in light propagating in nonlinear media. While spatial confinement turns photons into massive particles, mixing of light with matter degrees of freedom (polaritons) provides effective photon-photon interactions. In semiconductor microcavities, for instance, gases of exciton-polaritons undergo Bose-Einstein condensation [13–16] and the study of superfluidity [17–19], vortices [20] or solitons [21] in these quantum fluids of light [22] has been the subject of great scientific interest.

Yet in the context of nonlinear optics, a rather different approach to quantum fluids of light arises in bulk nonlinear media under paraxial optical propagation. In these geometries, the two-dimensional transverse dynamics of light obeys a nonlinear Schrödinger (NLS) equation similar to the Gross-Pitaevskii equation for the macroscopic wavefunction of a weakly interacting Bose gas [1], where the time evolution is mapped onto the longitudinal propagation, corresponding to a conservative (Hamiltonian) dynamics in these transformed coordinate system. Many interesting effects have been observed under such paraxial geometries, namely the formation of non-dissipative shock-waves [23, 24] and vortices [25], Rayleigh-Taylor instabilities [26], superfluid flow [27–29] and kinetic Bose-Einstein condensation [30].

Here, we describe the onset of a two-stream instability, analogous to similar kinetic processes in plasma physics, when two counter-flowing fluids interact via the optical nonlinearity, under the paraxial geometry setting - see Fig. (1). We begin by introducing the hydrodynamic model of the two-dimensional optical fluid and analyze its dispersion and stability. Under specific conditions, an instability can be triggered, rooted in the resonant energy transfer from the drift velocity to the elementary (Bogoli-

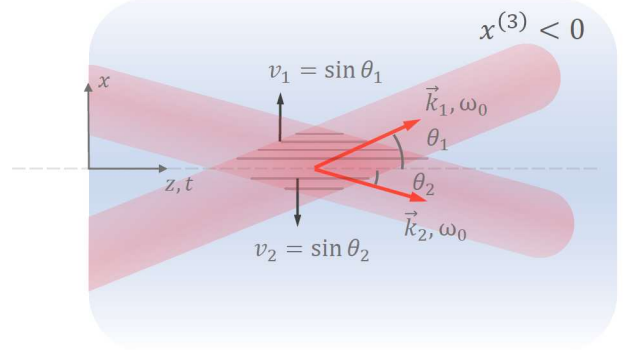


FIG. 1. (color online) Schematic representation of the two-stream instability, in self-defocusing optical media ($\chi^{(3)} < 0$). Under paraxial propagation, the time evolution of the two-dimensional optical fluid, in the transverse (x, y) plane, is mapped onto the strong (longitudinal) propagation direction. The flow speed v (in the transverse plane) is set by the propagation angle, namely $v = \sin \theta$. In the region where the two flows interact, a kinetic instability arises due to the resonant energy transfer from the stream to the elementary excitations on top of the optical fluid.

ubov) excitations of the photon gas. The unstable regime is described in detail and its experimental realization is discussed.

Optical Hydrodynamic Theory - The nonlinear propagation of an optical field (ignoring polarization degrees of freedom) is generally described by the wave equation

$$\left(\nabla^2 - \frac{1}{c^2} \frac{\partial^2}{\partial t^2} \right) E(\mathbf{r}, t) = \mu_0 \frac{\partial^2}{\partial t^2} P(\mathbf{r}, t), \quad (1)$$

with $E(\mathbf{r}, t)$ the electric field, $c = (\epsilon_0 \mu_0)^{-1/2}$ the speed of light and ϵ_0 the electric permittivity in vacuum. The polarization P of a generic Kerr medium is given by $P = \epsilon_0 \chi^{(1)} E + \epsilon_0 \chi^{(3)} |E|^2 E$, with $\chi^{(1)}$ and $\chi^{(3)}$ the linear and third order (Kerr) susceptibilities, respectively, the latter quantifying the strength of the optical nonlinearity. Usually, $\chi^{(1)} = \chi_0^{(1)} + \delta \chi^{(1)}(\mathbf{r})$ may be a function of the spatial coordinates, giving rise to an external potential. Let us consider a monochromatic carrier wave

of frequency ω_0 paraxially propagating along the z direction, $E(\mathbf{r}, t) = \psi(\mathbf{r}_\perp, z)e^{i\omega_0 t - ik_0 z}$, with $\mathbf{r}_\perp = (x, y)$, $k_0 = \omega_0/c$ the vacuum wavenumber of the carrier wave and $n = \sqrt{1 + \chi_0^{(1)}}$ the homogeneous linear index of refraction. The slowly varying complex field amplitude $\psi(\mathbf{r}_\perp, z)$ obeys the nonlinear Schrödinger (NLS) equation

$$i\frac{\partial\psi}{\partial z} = -\frac{1}{2nk_0}\nabla_\perp^2\psi - \frac{k_0}{2n}\left[\delta n^2(\mathbf{r}_\perp) + \chi^{(3)}|\psi|^2\right]\psi, \quad (2)$$

describing the dynamics of bosonic quasi-particles which acquire an effective mass $m_{\text{eff}} = \hbar^2 nk_0$ due to the transverse confinement inherent to the paraxial approximation. The perturbations on the linear index of refraction have been defined as $\delta n^2 = \delta\chi^{(1)}$. The paraxial approximation is rooted in the idea that the spatial variations of the field envelope are much slower than those of the carrier wave, and that transverse dynamics is highly suppressed. Its accuracy is verified as long as $\frac{|\nabla_\perp^2\psi|}{k_0^2} \sim \frac{|\partial\psi/\partial z|}{k_0} \ll 1$.

In the NLS equation above, the temporal evolution of ψ has been mapped onto the spatial propagation along the z direction. The perturbations on the linear index of refraction provide an external potential $V_0(\mathbf{r}_\perp) = -\frac{k_0}{2n}\delta n^2(\mathbf{r}_\perp)$, where an higher (lower) refractive index induces confining (repulsive) forces. These can be generated either by local structuring the physical and/or chemical properties of the medium, or by optically inducing refractive index modulations. The optical nonlinearity is at the origin of contact interactions of strength $g = -\frac{k_0}{2n}\chi^{(3)}$ and the local photon-photon potential $V(\mathbf{r}_\perp, z) = g|\psi(\mathbf{r}_\perp, z)|^2$, such that for $\chi^{(3)} > 0$ ($\chi^{(3)} < 0$) - photons experience attractive (repulsive) interactions.

In the paraxial geometry, the transverse flow speed (across the x direction, for instance) can be defined as $v = p_x/m_{\text{eff}}$, with $p_x = \hbar k_x$ a small photon momentum in the x direction, compliant with the paraxial approximation. Together with the definition of the effective photon mass, $v = k_x/nk_0$ or, in terms of the propagation angle θ , $v = \sin\theta = n^{-1}\sin\theta_i$, where the last equality follow from Snell's refraction law and θ_i the incidence angle. Due to the $t \leftrightarrow z$ mapping, flow speeds are expressed as adimensional quantities, corresponding to angles of propagation and quantifying transverse to longitudinal propagation.

An optical hydrodynamic description, equivalent to the NLS equation, begins the Madelung transformation, explicitly separating the complex amplitude of the optical field into its (real) amplitude and phase components, $\psi = \sqrt{\rho}e^{i\phi}$. From here, the definition of the fluid density (light intensity) and velocity field follows as $\rho = |\psi|^2$ and $\mathbf{v} = \nabla_\perp\phi$, respectively, the latter consistent with the eikonal intuition of energy transport normal to the wavefront. These quantities satisfy the hydrodynamic

equations

$$\frac{\partial\rho}{\partial z} + \nabla_\perp(\rho\mathbf{v}) = 0, \quad \text{and} \quad (3)$$

$$\frac{\partial\mathbf{v}}{\partial z} + (\mathbf{v} \cdot \nabla_\perp)\mathbf{v} = -g\nabla_\perp\rho + \frac{1}{2}\nabla_\perp\left(\frac{1}{\sqrt{\rho}}\nabla_\perp^2\sqrt{\rho}\right), \quad (4)$$

where the coordinates have been rescaled accordingly to $(x, y, z) \rightarrow nk_0(x, y, z)$. These are the usual continuity and Navier-Stokes equations of fluid mechanics. The wave character manifests itself through the last term in Eq. (4), usually referred to as the Bohm potential or quantum pressure, and is responsible for the non-local behavior and Heisenberg-like uncertainty associated with ondulatory systems.

Two-Stream Instability - We now turn to the case of two optical fluids where, without loss of generality, one shall be considered to be at rest, while the other is flowing with a velocity \mathbf{v}_0 . The hydrodynamic quantities can be expanded accordingly to $\rho_{1,2} = \rho_0 + \delta\rho_{1,2}$, $\mathbf{v}_1 = \delta\mathbf{v}_1$, $\mathbf{v}_2 = \mathbf{v}_0 + \delta\mathbf{v}_2$ and the corresponding governing equations linearized by retaining only first order terms in the perturbations. The linearized dynamics are evaluated by Fourier decomposition, $\delta\rho_{1,2}(\mathbf{r}_\perp, z) = A_{1,2}e^{i\mathbf{q}\cdot\mathbf{r}_\perp - i\Omega z}$, with A_i the mode amplitude and \mathbf{q} and Ω the transverse wavevector and frequency of the elementary excitations, respectively, related by the dispersion relation

$$1 - \frac{1}{2}c_s^2q^2\left[\frac{1}{\Omega^2 - q^4/4} + \frac{1}{(\Omega - \mathbf{v}_0 \cdot \mathbf{q})^2 - q^4/4}\right] = 0, \quad (5)$$

with $c_s = \sqrt{2\rho_0g}$. We begin by noting that, for a single optical component with zero drift velocity,

$$\Omega^2 = c_s^2q^2 + \frac{1}{4}q^4. \quad (6)$$

The latter is equivalent to the Bogoliubov dispersion relation of a weakly interacting Bose gas. For low momenta, it describes acoustic behavior, $\Omega \simeq c'_s q$, with $c'_s = \sqrt{g\rho_0}$ the single component speed of sound which, in terms of the optical parameters, $c'_s = n^{-1}\sqrt{-\chi^{(3)}|E_0|^2/2}$. Due to the $t \leftrightarrow z$ mapping, Ω has units of inverse length with the speed of sound becoming an adimensional quantity, for the same reasons as before. The linear dispersion is at the origin of superfluidity in these systems [29, 31]. This emergent behavior, phenomenologically described by Landau's critical velocity criteria, is microscopically related with suppression of radiation pressure forces [28]. In the self-focusing case ($\chi^{(3)} > 0$), the flow is unstable, corresponding to the emergence of an imaginary root in the Bogoliubov dispersion, eventually resulting in the filamentation of the optical stream. For high momenta, the acoustic dispersion gives way to a single-particle behavior, with a parabolic dispersion $\Omega \simeq q^2/2$, due to the transverse photon mass. The breakdown of fluid

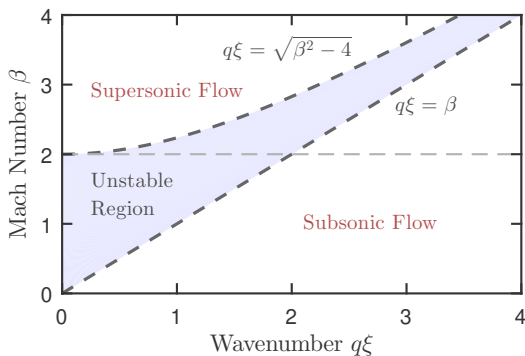


FIG. 2. (color online) Stability diagram in the $(q\xi, \beta)$ plane. The upper subplane ($\beta > 2$) defines the region of supersonic flows, while the lower part ($\beta < 2$) depicts the subsonic regime, where a dynamical instability is expected for low wavenumbers.

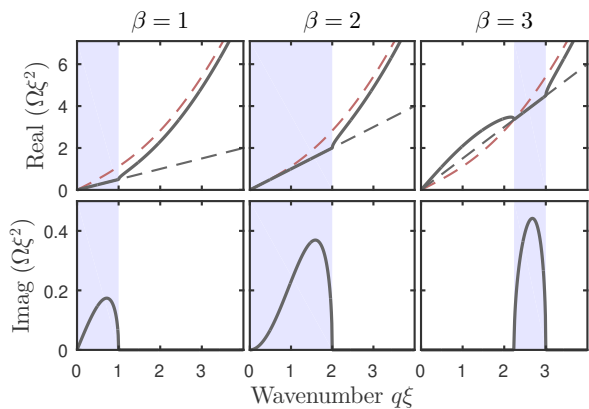


FIG. 3. (color online) Real (top row) and imaginary part (bottom row) of the dispersion relation of two coupled optical fluids. The full black line depicts the unstable mode, while, for the sake of reference, the red and black dashed lines represent both the Bogoliubov dispersion and the streaming term $\Omega\xi^2 = \beta(q\xi)/2$. From left to right $\beta = 1$ (subsonic), $\beta = 2$, $\beta = 3$ (supersonic) and the shaded area marks the unstable region.

behavior, corresponding to the transition from acoustic (phonon) to single-particle (massive photon) regime occurs approximately at $q \sim \xi^{-1}$, with $\xi = c_s^{-1}$ the healing length, in analogy with Bose-Einstein condensates. In regular units and in terms of the optical parameters, $\xi = k_0^{-1} \sqrt{-2/(\chi^{(3)}|E_0|^2)}$. The optical nonlinearity is at the origin of the acoustic behavior at low momenta and, for $\chi^{(3)} \rightarrow 0$ the speed of sound vanishes while the healing length diverges, corresponding to single particle (photon) dispersion in the entire spectrum. It is also worth mentioning the case of a single optical fluid with drift velocity \mathbf{v}_0 , with the modified dispersion relation $(\Omega - \mathbf{v}_0 \cdot \mathbf{q})^2 = c_s'^2 q^2 + \frac{1}{4} q^4$, corresponding to a simple Doppler-shift of the mode frequency.

We now turn to the full dispersion relation in Eq. (5),

with solutions given by

$$\Omega\xi^2 = \frac{1}{2} (q\xi) \left[\beta \pm \sqrt{2 + \beta^2 + (q\xi)^2 \pm 2\sqrt{1 + 2\beta^2 + \beta^2 (q\xi)^2}} \right], \quad (7)$$

with the Mach number defined as $\beta = v_0/c_s$. Unstable modes (complex roots) exists in two distinct regimes - see Fig. (2). On the one hand, for subsonic flows, defined here as $\beta < 2$, unstable excitations exist for all wavenumbers satisfying $0 < q\xi < \beta$. In regular units, the latter translates to $0 < q < nk_0 \sin \theta$ - a transverse instability will be verified at all wavenumbers smaller than that of the carrier wave projected onto the transverse subspace. At the instability boundary, when $q = nk_0 \sin \theta$, the momentum of the collective mode on top of the optical fluid, $\hbar q$, is the same equals that of the traveling photon in the transverse direction, at which point the former can no longer be excited by the latter and the instability vanishes. On the other hand, in the supersonic regime ($\beta \geq 2$), the instability is contained within the spectral region $\sqrt{\beta^2 - 4} < q\xi < \beta$. While the upper boundary is equivalent to the subsonic case, a lower cut-off in the unstable region emerges here, given by the condition of resonance between the optical stream and the Bogoliubov waves, namely $\beta(q\xi)/2 = \Omega_B$, with $\Omega_B^2 = (q\xi)^2 + 1/4 (q\xi)^4$ and, only modes with wavenumber higher than the resonant case become unstable.

The behavior of the dispersion relation in both sub and supersonic regimes is depicted in see Fig. (3). While in the stable region the waves in the resting fluid are described by the Bogoliubov dispersion, the unstable modes acquire the character of the optical stream (linear dispersion). For high Mach numbers the unstable region at high momenta narrows and, at the limit $\beta \rightarrow \infty$ the fluid is always stable. The instability is then fully rooted in the acoustic dispersion and fluid-like properties induced by photon-photon interactions. In plasma physics, two-stream instabilities occurs when travelling electrons couple via electrostatic interactions with an ionic background [32]. These instabilities, often interpreted as inverse Landau damping, generally demand kinetic formulations in both real and momentum (phase) space. The latter is equivalently mimicked here with hydrodynamic equations for a two-component fluid with different streaming velocities. A full quantum kinetic description can be constructed in terms of a Wigner distribution function whose evolution is equivalent to the NLS equation [33, 34], which may be an appropriate formulation of quantum wave turbulence. Also, while the present two-stream instability is rooted in the resonant transfer of kinetic energy from the streaming flow into the Bogoliubov modes on top of the optical fluid, the recently observed Rayleigh-Taylor instability [26] originates from

the shear associated with two optical fluids with different densities (intensities) being accelerated towards each other.

Experimental Considerations - Among the platforms where the analogy between paraxial propagation and quantum fluids of light has been investigated, nonlinear crystals have attracted particular interest [23, 26, 30]. Atomic vapors driven in the vicinity of a sharp electronic resonance offer yet a different approach which has been greatly unexplored. Few examples include the observation self-focusing and self-trapping effects [35, 36]. Here, the (linear) two-level susceptibility is given by

$$\chi = -\frac{\mu^2 n_a^2}{\hbar \epsilon_0} \frac{\delta - i\Gamma/2}{\delta^2 + \Gamma^2/4 + \Omega_R^2/2}, \quad (8)$$

with $\mu = -\langle g|er|e \rangle$ the matrix element of the dipole transition, e the electron charge, n_a the atomic density, $\delta = \omega_0 - \omega_a$ the detuning from resonance, $\Gamma = 1/\tau$ the linewidth of the atomic transition (τ the lifetime of the excited state) and $\Omega_R = \mu E_0/\hbar$ the Rabi frequency quantifying the coupling strength. Although higher susceptibilities are achieved close to resonance, undesired photon losses are also maximized here. Far-from-resonance ($|\delta| \gg \Gamma$) propagation mitigates the dispersive response and the imaginary part of the susceptibility can be dropped. Nonlinear propagation arises due to saturation of the atomic transition (originating from the finite lifetime of the excited state) and the dependence of the susceptibility on the electric field amplitude (via the Rabi frequency). We can define the saturation intensity I_s as $I/I_s = \Omega_R^2/2\delta^2$, with $I_s = 4(\delta/\Gamma)^2 I_s^0$ and $I_s^0 = c\epsilon_0 \hbar^2 \Gamma^2 / 4\mu^2$ the saturation intensity close to resonance. Moreover, considering a refractive index of the form $n = n_0 + n_2 I$ and assuming $I \ll I_s$, we can expand Eq. (8) to first order in I/I_s , yielding

$$n_0 = 1 - \frac{n_a \mu^2}{2\epsilon_0 \hbar \Gamma} \frac{1}{\delta/\Gamma}, \quad \text{and} \quad n_2 = \frac{n_a \mu^4}{2c\epsilon_0^2 \hbar^3 \Gamma^3} \frac{1}{(\delta/\Gamma)^3}. \quad (9)$$

The sign of the optical nonlinearity depends on which side the atomic transition is driven. Particularly, for red-detuned driving ($\delta < 0$) the atomic gas behaves as a self-defocusing medium ($n_2 < 0$). The Kerr approximation is relevant as long as the limit $I/I_s \ll 1$ is verified, otherwise higher order expansions are in order. Here, saturation and the corresponding nonlinear effects emerge at low intensities due to the resonant enhancement of the interaction [37]. The calculation of the Kerr index for a gas of ^{85}Rb is depicted in Fig. (4). As an example, for a vapor of density $n_0 = 10^{12} \text{ cm}^{-3}$ driven at $\delta = -120 \text{ MHz}$ (approximately -20Γ), such that $|\delta| \gg \Gamma$ and losses can be ignored, we obtain the Kerr index $n_2 \simeq -7.5 \times 10^{-5} \text{ cm}^2/\text{W}$, saturation intensity $I_s \simeq 4 \text{ W}/\text{cm}^2$ and a linear index of refraction close to unit, $n_0 \simeq 1$. Assuming linearly polarized light of intensity $I = 0.4 \text{ W}/\text{cm}^2$, such that $I/I_s \simeq 0.1 \ll 1$ (Kerr approximation) yields a modulation of the index of refraction $|\Delta n| \simeq 3 \times 10^{-5}$. In

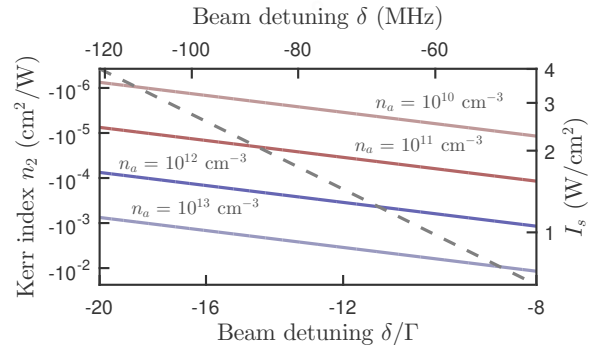


FIG. 4. (color online) (Left-axis, full lines) Kerr index for the D2 line of ^{85}Rb , at approximately 780 nm, as a function of δ and for different atomic densities. The effective far-detuned dipole moment (accounting for the multilevel hyperfine structure of Rubidium) $\mu = 2.069 \times 10^{-29} \text{ C}\cdot\text{m}$ (for linearly polarized light) and the transition linewidth $\Gamma = 2\pi \times 6.06 \text{ MHz}$ [40]. (Right-axis, dashed line) Effective saturation intensity $I_s = 4(\delta/\Gamma)^2 I_s^0$ for far-detuned light, with $I_s^0 = 2.5 \text{ mW}/\text{cm}^2$ [40].

order to probe the acoustic range ($q\xi \ll 1$) light must propagate long enough such that at least one oscillation period (of the Bogoliubov modes) is observed. Equivalently, one may impose the condition $d \gg c_s(c\Delta t)$, demanding a sample of length $l = (c/n_0)\Delta t \gg \xi/(n_0 c_s)$ or, translating into regular units, $l \gg \lambda_0/\Delta n$. Assuming the same Kerr index obtained before, for the D2 line of ^{85}Rb at approximately 780 nm, one obtains $\lambda/\Delta n \simeq 26 \text{ mm}$ and samples of the order of 10-20 cm long are required, although this condition may be softened in some cases [29]. The two-stream instability may be diagnosed by imaging the light exiting the nonlinear medium with a CCD camera, either in real or Fourier space (far-field imaging). The latter provides direct access to the wavenumber of the unstable modes, facilitating the comparison with the theoretical model. The development of the instability shall encompass the excitation of quantum superfluid turbulence. The turbulent velocity field (phase gradient) can be investigated by interfering the output light with a reference plane wave (hologram) [26]. In scenarios of developed turbulence, quantum vortices (phase discontinuities) manifest as fork-like dislocations in the interference pattern [20, 21, 38]. Statistical analysis of the velocity field may required the measurement of the full phase map, which can be retrieved with phase shifting holography [30, 39].

Conclusion - In summary, we described a two-stream instability in paraxial optical fluids. The ratio between the flow velocity and the speed of sound of the collective Bogoliubov excitations can be precisely controlled either via the optical propagation angle or the background light intensity, which can be used to selectively excite a particular spectral region and probe the dispersion relation of the quantum optical fluid. The class of instabilities

described here may also provide a route to the generation of topological structures such as vortices and solitons in quantum gases. Moreover, they may play an important role in the investigation of general out-of-equilibrium phenomena in the superfluid regime and, in particular, in the excitation of quantum turbulence, presenting an opportunity to probe processes of energy transfer between different scales and the emergence of turbulent cascades [9, 10, 12, 41, 42].

JDR acknowledges the financial support of FCT - Fundação da Ciência e Tecnologia through the grant number SFRH/BD/52323/2013. Stimulating discussions with Hugo Terças are also acknowledged.

* Corresponding author:joadmrodrigues@tecnico.ulisboa.pt

- [1] F. Dalfovo, S. Giorgini, L. P. Pitaevskii, and S. Stringari, *Rev. Mod. Phys.* **71**, 463 (1999).
- [2] A. J. Leggett, *Rev. Mod. Phys.* **73**, 307 (2001).
- [3] W. Ketterle, *Rev. Mod. Phys.* **74**, 1131 (2002).
- [4] R. Onofrio, C. Raman, J. M. Vogels, J. R. Abo-Shaer, A. P. Chikkatur, and W. Ketterle, *Phys. Rev. Lett.* **85**, 2228 (2000).
- [5] P. Engels and C. Atherton, *Phys. Rev. Lett.* **99**, 160405 (2007).
- [6] T. W. Neely, E. C. Samson, A. S. Bradley, M. J. Davis, and B. P. Anderson, *Phys. Rev. Lett.* **104**, 160401 (2010).
- [7] R. Desbuquois, L. Chomaz, T. Yefsah, J. Leonard, J. Beugnon, C. Weitenberg, and J. Dalibard, *Nat Phys* **8**, 645 (2012).
- [8] J. Yepez, G. Vahala, L. Vahala, and M. Soe, *Phys. Rev. Lett.* **103**, 084501 (2009).
- [9] D. I. Bradley, S. N. Fisher, A. M. Guenault, R. P. Haley, G. R. Pickett, D. Potts, and V. Tsepelin, *Nat Phys* **7**, 473 (2011).
- [10] A. S. Bradley and B. P. Anderson, *Phys. Rev. X* **2**, 041001 (2012).
- [11] S. K. Nemirovskii, *Physics Reports* **524**, 85 (2013), quantum Turbulence: Theoretical and Numerical Problems.
- [12] N. Navon, A. L. Gaunt, R. P. Smith, and Z. Hadzibabic, *Nature* **539**, 72 (2016), letter.
- [13] J. Kasprzak, M. Richard, S. Kundermann, A. Baas, P. Jeambrun, J. M. J. Keeling, F. M. Marchetti, M. H. Szymanska, R. Andre, J. L. Staehli, V. Savona, P. B. Littlewood, B. Deveaud, and L. S. Dang, *Nature* **443**, 409 (2006).
- [14] H. Deng, D. Press, S. Götzinger, G. S. Solomon, R. Hey, K. H. Ploog, and Y. Yamamoto, *Phys. Rev. Lett.* **97**, 146402 (2006).
- [15] M. Wouters and I. Carusotto, *Phys. Rev. Lett.* **99**, 140402 (2007).
- [16] H. Deng, H. Haug, and Y. Yamamoto, *Rev. Mod. Phys.* **82**, 1489 (2010).
- [17] I. Carusotto and C. Ciuti, *Phys. Rev. Lett.* **93**, 166401 (2004).
- [18] A. Amo, J. Lefrere, S. Pigeon, C. Adrados, C. Ciuti, I. Carusotto, R. Houdre, E. Giacobino, and A. Bramati, *Nat Phys* **5**, 805 (2009).
- [19] A. Amo, D. Sanvitto, F. P. Laussy, D. Ballarini, E. d. Valle, M. D. Martin, A. Lemaître, J. Bloch, D. N. Krizhanovskii, M. S. Skolnick, C. Tejedor, and L. Vina, *Nature* **457**, 291 (2009).
- [20] K. G. Lagoudakis, M. Wouters, M. Richard, A. Baas, I. Carusotto, R. Andre, L. S. Dang, and B. Deveaud-Pledran, *Nat Phys* **4**, 706 (2008).
- [21] A. Amo, S. Pigeon, D. Sanvitto, V. G. Sala, R. Hivet, I. Carusotto, F. Pisanello, G. Leménager, R. Houdré, E. Giacobino, C. Ciuti, and A. Bramati, *Science* **332**, 1167 (2011).
- [22] I. Carusotto and C. Ciuti, *Rev. Mod. Phys.* **85**, 299 (2013).
- [23] W. Wan, S. Jia, and J. W. Fleischer, *Nat Phys* **3**, 46 (2007).
- [24] S. Jia, W. Wan, and J. W. Fleischer, *Phys. Rev. Lett.* **99**, 223901 (2007).
- [25] G. A. Swartzlander and C. T. Law, *Phys. Rev. Lett.* **69**, 2503 (1992).
- [26] S. Jia, M. Haataja, and J. W. Fleischer, *New Journal of Physics* **14**, 075009 (2012).
- [27] P. Leboeuf and S. Moulieras, *Phys. Rev. Lett.* **105**, 163904 (2010).
- [28] P.-E. Larré and I. Carusotto, *Phys. Rev. A* **91**, 053809 (2015).
- [29] D. Vocke, T. Roger, F. Marino, E. M. Wright, I. Carusotto, M. Clerici, and D. Faccio, *Optica* **2**, 484 (2015).
- [30] C. Sun, S. Jia, C. Barsi, S. Rica, A. Picozzi, and J. W. Fleischer, *Nat Phys* **8**, 470 (2012).
- [31] I. Carusotto, *Proceedings of the Royal Society of London A: Mathematics and Physics* **468**, 1001 (2012).
- [32] D. R. Nicholson, *Introduction to Plasma Theory* (Wiley, New York, 1983).
- [33] J. Mendonça, A. Serbeto, and P. Shukla, *Physics Letters A* **372**, 2311 (2008).
- [34] H. Terças, J. T. Mendonça, and G. R. M. Robb, *Phys. Rev. A* **79**, 065601 (2009).
- [35] D. Grischkowsky, *Phys. Rev. Lett.* **24**, 866 (1970).
- [36] J. E. Bjorkholm and A. A. Ashkin, *Phys. Rev. Lett.* **32**, 129 (1974).
- [37] C. F. McCormick, D. R. Solli, R. Y. Chiao, and J. M. Hickmann, *Phys. Rev. A* **69**, 023804 (2004).
- [38] S. Inouye, S. Gupta, T. Rosenband, A. P. Chikkatur, A. Görlitz, T. L. Gustavson, A. E. Leanhardt, D. E. Pritchard, and W. Ketterle, *Phys. Rev. Lett.* **87**, 080402 (2001).
- [39] I. Yamaguchi and T. Zhang, *Opt. Lett.* **22**, 1268 (1997).
- [40] D. A. Steck, *Rubidium 85 D Line Data* (2013).
- [41] M. T. Reeves, T. P. Billam, B. P. Anderson, and A. S. Bradley, *Phys. Rev. Lett.* **110**, 104501 (2013).
- [42] T. W. Neely, A. S. Bradley, E. C. Samson, S. J. Rooney, E. M. Wright, K. J. H. Law, R. Carretero-González, P. G. Kevrekidis, M. J. Davis, and B. P. Anderson, *Phys. Rev. Lett.* **111**, 235301 (2013).